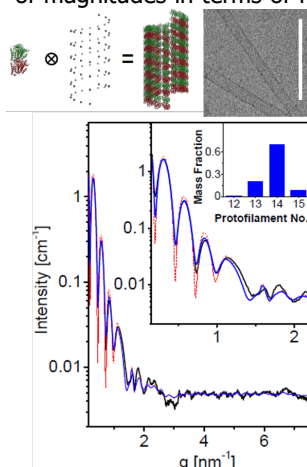


### Dynamics of tubulin nucleation and assembly

Tubulin assembles and disassembles into microtubule (MT) and multiple dynamic structures exhibiting complex behavior. MT assembly requires GTP-bound- $\alpha\beta$ -tubulin, and GTP hydrolysis by  $\beta$ -tubulin (into GDP) is required to generate dynamic MTs, operating out-of-equilibrium. Tubulin nucleation and MT assembly are highly abundant and important processes in cytoskeleton biology but poorly understood because the assembly is stochastic, occurs in solution, and involves GTP hydrolysis. In relevant solution conditions, structural information at high spatial and temporal resolutions is required to determine the underlying physics leading to the highly dynamic tubulin structures. Tubulin structures are often too dynamic, soft, and large in molecular weight to be crystallized. Therefore, we have used time-resolved X-ray scattering at ID02 beamline to study tubulin assemblies in solution. Cryo-TEM and various biophysical and biochemical methods often supported the scattering measurements. We have studied the structures and intermolecular interactions in these complex, weakly ordered, and dynamic self-assembling structures by applying state-of-the-art data analysis integrated with simulations, theory, and various algorithms. **Our lab has developed the skills to study tubulin and MTs in their natural dynamic states.** We have developed our experimental protocols to purify tubulin<sup>1</sup> and study the high-resolution structure and dynamics of tubulin and MT<sup>1-2</sup> in their natural state (Figure 1) and in the presence of ions<sup>3</sup>.

In 2019, we have published our new **groundbreaking** software paper<sup>4</sup> for **solution X-ray scattering data analysis from large and complex macromolecular assemblies**. The program, called **D+**, is comprehensive software using our cutting-edge state-of-the-art **algorithms**, containing more than **100,000 lines of open-source C++ and CUDA codes**, running on both CPU and GPU platforms. The capabilities of **D+** exceeds earlier programs by several orders of magnitudes in terms of flexibility and complexity of the modeled structures and computation speed (see Figure 7 in <sup>4</sup>). In **D+**, atomic or geometric models are docked into their assembly symmetry, describing how subunits repeat in a complex structure. This can be done hierarchically, in a bottom-up approach, for many different subunits. In that way, **D+** can define any macromolecular assembly structure and compute its solution X-ray scattering curve at high resolution. **D+** has a **python wrapper**, which allows its integration with simulations, theory, and a range of advanced optimization and signal processing algorithms, enabling it to attain unique dynamical and structural biophysical insight (see ref.<sup>1, 6-9</sup>). More recently, we have upgraded **D+** software to include many new python API functions, including structure factor and pair distribution function analyses and fiber-diffraction samples or structures in a single orientation<sup>10</sup>.

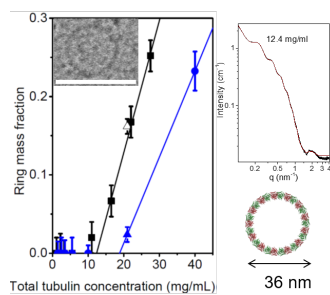


**Figure 1.** Dynamic microtubule (MT) in the presence of GTP<sup>2, 4-5</sup>. Cryo-TEM image of MT (scale bar equals 200 nm)<sup>2</sup>. Solution X-ray scattering data (black curve) and models<sup>4-5</sup>. In the red model, the atomic tubulin model (PDB 3J6F) was docked into the three-start left-handed helical MT lattice (a radius of 11.9 nm, and a pitch of 12.214 nm), containing 14 protofilaments, as illustrated in the cartoon. In the blue model, the mass fraction distribution of protofilaments, shown at the smaller inset, was taken into account. Both models were computed by **D+**, and the hydration layer of the entire MT structure was taken into account<sup>4-5</sup>.

The nucleation of tubulin and its assembly into MT were studied in the presence of excess GTP. Assembly was triggered by a temperature jump from 5 to 36°C and followed by time-resolved X-ray scattering. The assembly reactions start from a solution of cold (5°C) tubulin and end in a solution of tubulin at 36°C. At the end point MTs form and Figure 1 demonstrates that the end point of the reaction is well characterized. We have also been focusing on determining the ensembles of structures and intermolecular interactions in cold GTP/GDP-tubulin solutions, under a wide range of conditions. We found that in cold tubulin solutions, tubulin dimers coexisted with tubulin oligomers and (GDP-rich) tubulin single rings. The concentration of solution strongly depends on the GTP and GDP concentrations. We have therefore investigated the assembly and disassembly conditions for single tubulin rings and their relation to the kinetics of MT assembly and disassembly. We determined the structure of tubulin single rings using cryo-TEM and solution X-ray scattering<sup>1</sup>. The scattering curves were fitted to models of tubulin single rings, constructed by docking the atomic model of the dimer (PDB 3J6F or 1SA0) into the ring symmetry and by taking the hydration layer of the ring into account, using **D+**, (Figure 2). We found that there is a critical concentration for ring formation. The critical concentration increased with GTP concentration or with temperature. We have also found that during MT assembly, the fraction of rings and unassembled tubulin dimers simultaneously decreased. During MT disassembly, however, the mass fraction of dimers increased but the increase in the concentration of rings was delayed until the fraction of dimers was sufficiently high and crossed the critical concentration for ring formation<sup>1</sup>.

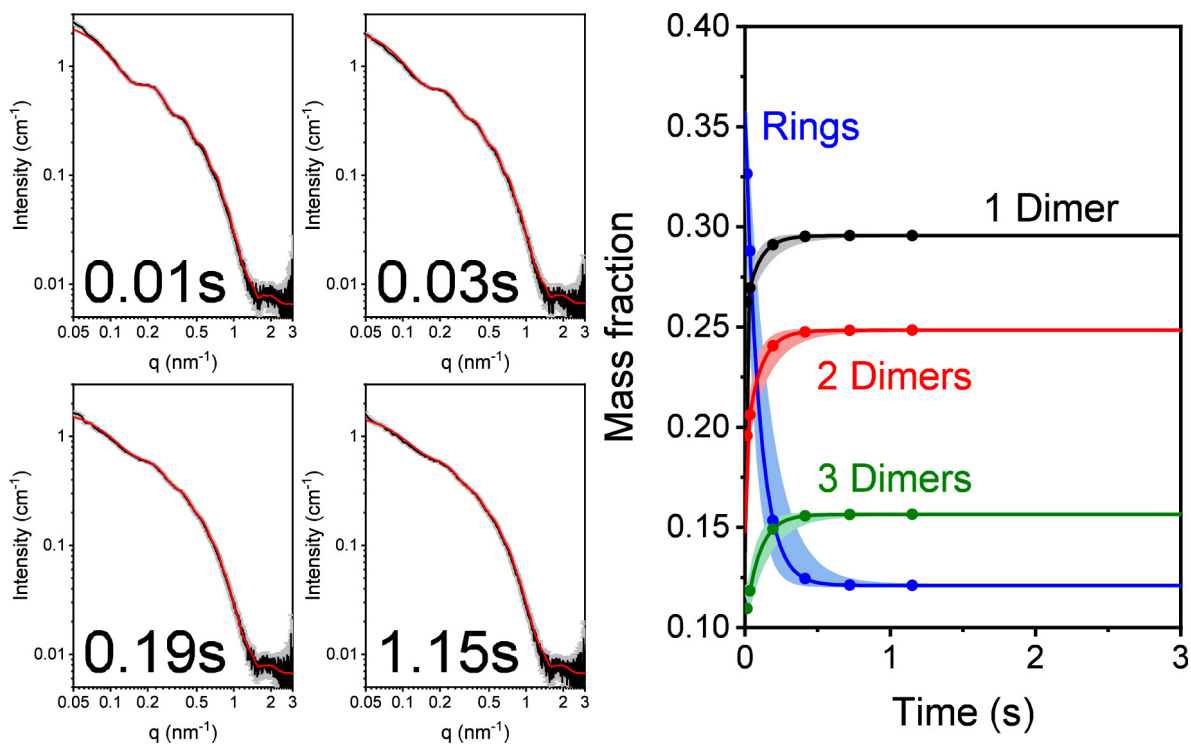
To resolve the ensemble of GTP and GDP-tubulin assemblies formed at low temperature, we have used off-line size exclusion chromatography (SEC) setup and analyzed the data of different fractions. We discovered that the solutions rapidly attained equilibrium (in the GDP-tubulin solution) or equilibrium-like state (in the GTP-tubulin solution). The entire SAXS data set were consistent with a thermodynamic model of tubulin single rings and curved tubulin oligomers.

The analysis revealed a dimer-dimer association free energy of  $-14.2$  and  $-13.2$   $k_B T$  for GDP- and GTP-tubulin, respectively. Surprisingly, in the solution of GDP-tubulin, we have also detected a small fraction of stable tubulin single rings, not predicted by the thermodynamic model. The radius of the rings was  $19.2$  nm. In the GTP solution, the fraction of stable rings was significantly lower.



**Figure 2.** Mass fraction of tubulin in ring structures as a function of the total tubulin concentration. GDP-rich tubulin solutions before GTP was added (black) and after 4 mM GTP were added (blue). Cryo-TEM image of a tubulin ring is also shown (scale bar equals 50 nm)<sup>1</sup>. The measured scattering curve (black) and the fitted model (red) are shown on the right. The computed model is based on the atomic dimer structure (PDB 1SA0) which was docked into the symmetry of the ring (see cartoon at the bottom). In addition to the ring structure, the mass fraction of all the tubulin oligomeric ring fractions were taken into account. The mass fraction of all the tubulin assemblies was computed based on a thermodynamic model of macromolecular assemblies, based on which the dimer-dimer association free energy ( $-14.2$   $k_B T$  for GDP tubulin and  $-13.2$   $k_B T$  for GTP tubulin) was obtained by fitting the model to the scattering data. The paper describing the analysis is under preparation.

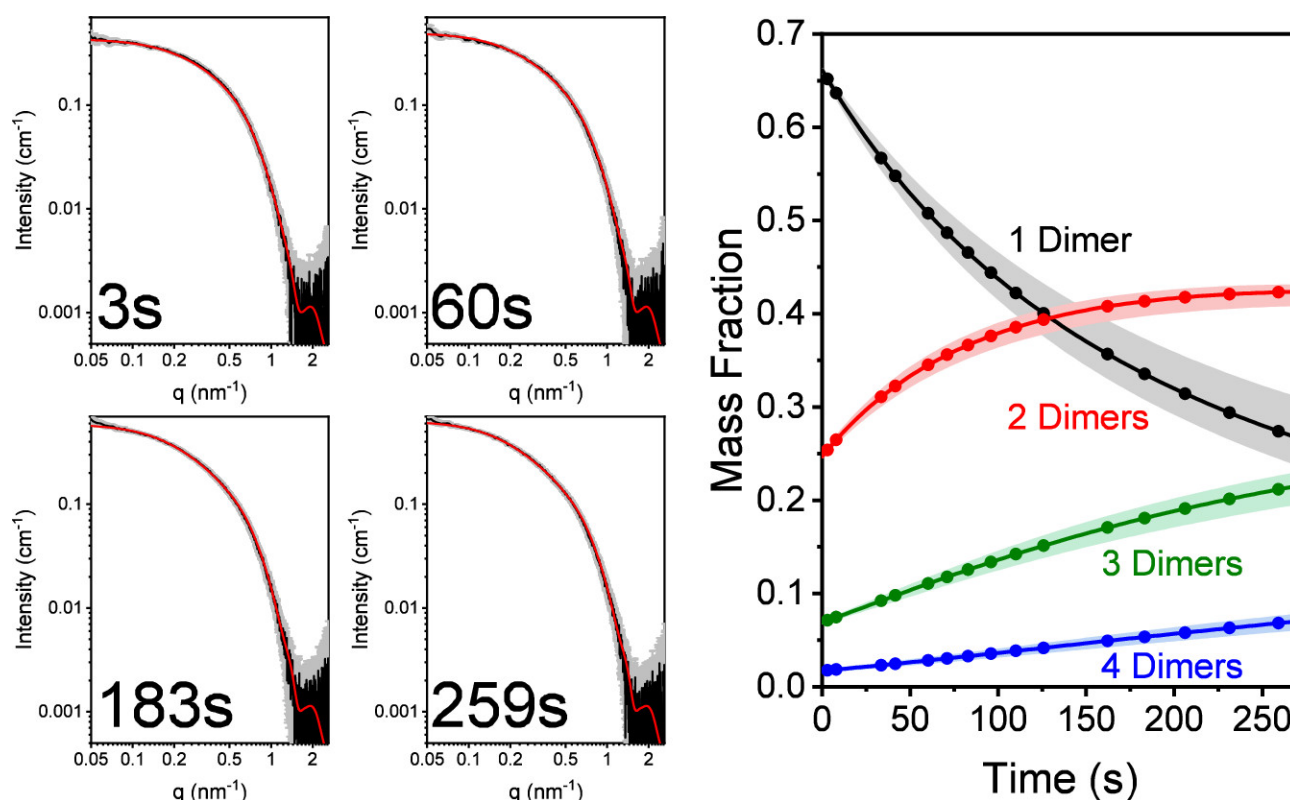
Using the state-of-the-art solution synchrotron time-resolved small-angle X-ray scattering (TR-SAXS) at ID02, we discovered a disassembly catastrophe (half-life of  $\sim 0.1$  s) of tubulin rings and oligomers upon dilution or addition of GTP (Figure 3). The TR-SAXS data were fit to an isodesmic kinetic model, in which dimers were rapidly added or removed one at a time and rings were closed or opened at a rate that was 2 orders of magnitude slower. The thermodynamic parameters determined by the steady-state measurements and SEC-SAXS chromatogram analysis<sup>11</sup> were used to estimate the initial size distribution and to calculate the ratio between the assembly and disassembly rate constants, according to the detailed balance conditions. The rate constants and the standard Helmholtz free energies used to analyze the TR-SAXS data are summarized in our paper<sup>12</sup>. A slower disassembly (half-life of  $\sim 38$  s) was observed following an increase in temperature. Our analysis showed that in all the cases, the assembly and disassembly processes were consistent with an isodesmic mechanism, involving a sequence of reversible reactions in which dimers were rapidly added or removed one at a time, terminated by a 2 order-of-magnitude slower ring-closing/opening step. We revealed how assembly conditions varied the mass fraction of tubulin in each of the coexisting structures, the rate constants, and the standard Helmholtz free energies for closing a ring and for longitudinal dimer-dimer associations<sup>12</sup>.



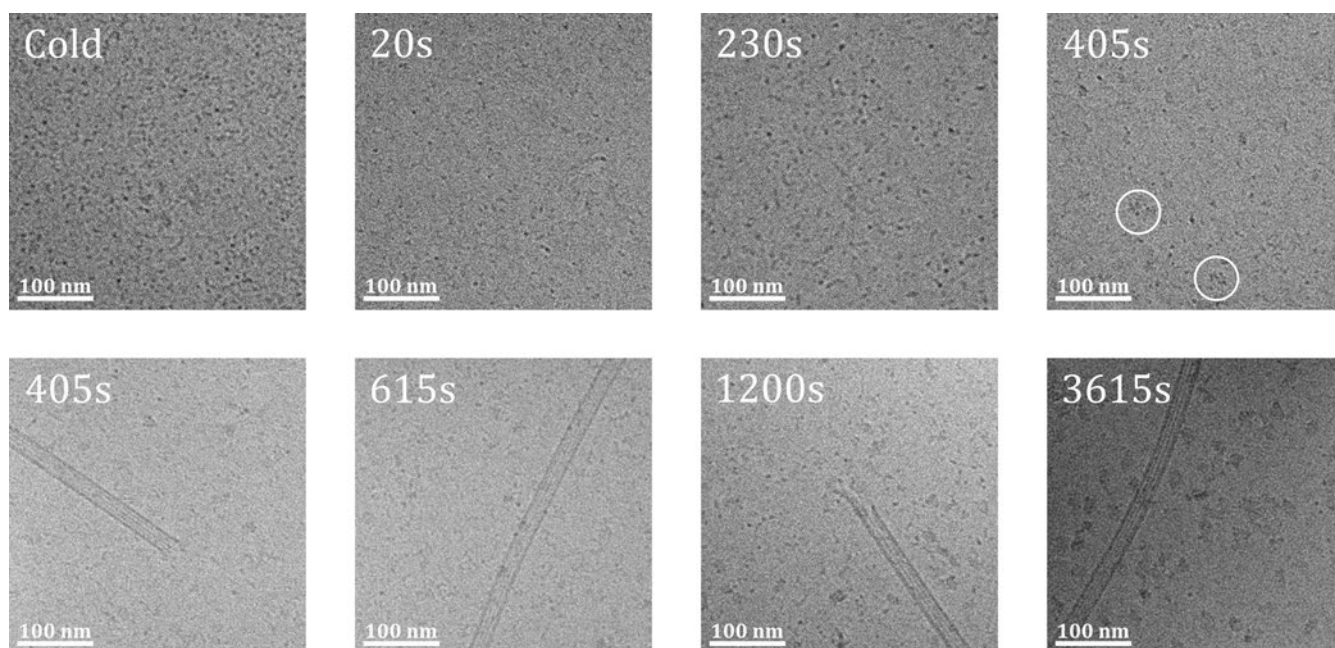
**Figure 3.** GDP-tubulin single-ring disassembly catastrophe following GTP addition. GDP-tubulin was mixed in a stopped-flow setup with BRB80, supplemented with  $8 \pm 0.5$  mM GTP. The four panels on the left present examples of TR-SAXS data (black curves, gray error bars) at selected time points, as indicated. The complete TR-SAXS data set is presented in

Figure S7. The data were fit (red curves) to an isodesmic kinetic model. The right panel shows the mass fraction of rings and ring fragments as a function of time.

Using SEC-eluted tubulin dimers in an assembly buffer solution free of glycerol and tubulin aggregates enabled us to start from a well-defined initial thermodynamic ensemble of isolated dynamic tubulin dimers and short oligomers. Following a temperature increase, time-resolved X-ray scattering and cryo-transmission electron microscopy during the initial nucleation phase revealed an isodesmic assembly mechanism of one-dimensional (1D) tubulin oligomers (where dimers were added and/or removed one at a time), leading to sufficiently stable two-dimensional (2D) dynamic nanostructures, required for MT assembly (Figure 4). A substantial amount of tubulin octamers accumulated before two-dimensional lattices appeared. Under subcritical assembly conditions, we observed a slower isodesmic assembly mechanism, but the concentration of 1D oligomers was insufficient to form the multistranded 2D nucleus required for MT formation (Figure 5)<sup>13</sup>.



**Figure 4.** Assembly kinetics above the critical MT assembly conditions. The panels on the left show the azimuthally integrated background-subtracted time-resolved scattering absolute intensity curves, at selected time points along the reaction (black curves and gray error bars), initiated by changing the temperature from 4 to 36 °C. The solid red curves are the best fit scattering intensity models. To model these data, we created a library of 1D curved oligomers by docking the atomic model of the tubulin dimer in a curved conformation (PDB entry 5JQG) into lattices of fragments of tubulin single rings with a radius of 19.2 nm. The right panel shows the computed mass fractions of the dominating assemblies as a function of time, based on the best fit rate constants (solid curves), where the shaded colored areas indicate the error in the mass fractions. The dots along the curves mark the time points at which TR-SAXS measurements were performed at ID02 beamline. A longer incubation time led to MT formation. The analysis of the entire TR-SAXS data set ( $\leq 259$  s, where the same kinetic model still applies) is presented in our publication<sup>13</sup>. The analysis was repeated using the straight conformation of the dimer (PDB entry 3JAT) in the assembly symmetry of straight 1D oligomers. This analysis led to a similar fit to the TR-SAXS data, slightly slower rate constants, and a stronger dimer–dimer self-association free energy.



**Figure 5.** Time-resolved cryo-TEM images of microtubule nucleation and assembly kinetics. A purified cold (4 °C) tubulin solution was filtered by SEC, and the dimer elution peak was collected at a concentration of  $70 \pm 5 \mu\text{M}$ , supplemented with  $4 \pm 1 \text{ mM}$  GTP, and incubated at 36 °C for the indicated durations. The change in temperature was performed by transferring 50  $\mu\text{L}$  of the cold tubulin solution to a heat block that was preheated to 36 °C. The shortest incubation time (20 s) was achieved by transferring a 2.5  $\mu\text{L}$  drop directly from the cold reservoir to the preheated cryo-TEM grid. White circles enclose coexisting 2D structures (at 405 s).

We have also investigated how the self-association of isolated tubulin dimers affects the rate of GTP hydrolysis and the equilibrium of nucleotide exchange. Both reactions are relevant for MT dynamics. We used HPLC to determine the concentrations of GDP and GTP and thereby the GTPase activity of SEC-eluted tubulin dimers in assembly buffer solution, free of glycerol and tubulin aggregates. When GTP hydrolysis was negligible, the nucleotide exchange mechanism was studied by determining the concentrations of tubulin-free and tubulin-bound GTP and GDP. We observed no GTP hydrolysis below the critical conditions for MT assembly (either below the critical tubulin concentration and/or at low temperature), despite the assembly of tubulin 1D curved oligomers and single-rings, showing that their assembly did not involve GTP hydrolysis. Under conditions enabling spontaneous slow MT assembly, a slow pseudo-first-order GTP hydrolysis kinetics was detected, limited by the rate of MT assembly. Cryo-TEM images showed that GTP-tubulin 1D oligomers were curved also at 36 °C. Nucleotide exchange depended on the total tubulin concentration and the molar ratio between tubulin-free GDP and GTP. We used a thermodynamic model of isodesmic tubulin self-association, terminated by the formation of tubulin single-rings to determine the molar fractions of dimers with exposed and buried nucleotide exchangeable sites (E-sites). Our analysis shows that the GDP to GTP exchange reaction equilibrium constant was an order-of-magnitude larger for tubulin dimers with exposed E-sites than for assembled dimers with buried E-sites. This conclusion may have implications on the dynamics at the tip of the MT plus end<sup>14</sup>.

## References

1. Shemesh, A.; Ginsburg, A.; Levi-Kalisman, Y.; Ringel, I.; Raviv, U., Structure, assembly, and disassembly of tubulin single rings. *Biochemistry* **2018**, *57* (43), 6153-6165.
2. Ginsburg, A.; Shemesh, A.; Millgram, A.; Dharan, R.; Levi-Kalisman, Y.; Ringel, I.; Raviv, U., Structure of dynamic, Taxol-stabilized, and GMPPCP-stabilized microtubule. *The Journal of Physical Chemistry B* **2017**, *121* (36), 8427-8436.
3. Raviv, D.; Asaf, S.; Abigail, M.; Yael, L.-K.; Israel, R.; Uri, R., *Hierarchical Assembly Pathways of Spermine Induced Tubulin Conical-Spiral Architectures*. 2020.
4. Ginsburg, A.; Ben-Nun, T.; Asor, R.; Shemesh, A.; Fink, L.; Tekoah, R.; Levartovsky, Y.; Khaykelson, D.; Dharan, R.; Fellig, A.; Raviv, U., D+: software for high-resolution hierarchical modeling of solution X-ray scattering from complex structures. *Journal of applied crystallography* **2019**, *52* (1), 219-242.
5. Ginsburg, A.; Ben-Nun, T.; Asor, R.; Shemesh, A.; Ringel, I.; Raviv, U., Reciprocal Grids: A Hierarchical Algorithm for Computing Solution X-ray Scattering Curves from Supramolecular Complexes at High Resolution. *Journal of Chemical Information and Modeling* **2016**, *56* (8), 1518-1527.

6. Asor, R.; Khaykelson, D.; Ben-nun-Shaul, O.; Oppenheim, A.; Raviv, U., Effect of Calcium Ions and Disulfide Bonds on Swelling of Virus Particles. *ACS omega* **2019**, *4* (1), 58-64.
7. Asor, R.; Selzer, L.; Schlicksup, C. J.; Zhao, Z.; Zlotnick, A.; Raviv, U., Assembly Reactions of Hepatitis B Capsid Protein into Capsid Nanoparticles Follow a Narrow Path Through a Complex Reaction Landscape. *ACS nano* **2019**.
8. Levartovsky, Y.; Shemesh, A.; Asor, R.; Raviv, U., Effect of Weakly Interacting Cosolutes on Lysozyme Conformations. *ACS Omega* **2018**, *3* (11), 16246-16252.
9. Louzon, D.; Ginsburg, A.; Schwenger, W.; Dvir, T.; Dogic, Z.; Raviv, U., Structure and intermolecular interactions between I-type straight flagellar filaments. *Biophysical journal* **2017**, *112* (10), 2184-2195.
10. Balken, E.; Ben-Nun, I.; Fellig, A.; Khaykelson, D.; Raviv, U., Upgrade of D+ software for hierarchical modeling of X-ray scattering data from complex structures in solution, fibers and single orientations. *Journal of Applied Crystallography* **2023**, *56* (4).
11. Shemesh, A.; Ginsburg, A.; Dharan, R.; Levi-Kalisman, Y.; Ringel, I.; Raviv, U., Structure and energetics of GTP-and GDP-tubulin isodesmic self-association. *ACS Chemical Biology* **2021**, *16* (11), 2212-2227.
12. Shemesh, A.; Ginsburg, A.; Dharan, R.; Levi-Kalisman, Y.; Ringel, I.; Raviv, U., Mechanism of tubulin oligomers and single-ring disassembly catastrophe. *The Journal of Physical Chemistry Letters* **2022**, *13* (23), 5246-5252.
13. Shemesh, A.; Dharan, N.; Ginsburg, A.; Dharan, R.; Levi-Kalisman, Y.; Ringel, I.; Raviv, U., Mechanism of the Initial Tubulin Nucleation Phase. *The Journal of Physical Chemistry Letters* **2022**, *13* (41), 9725-9735.
14. Shemesh, A.; Ghareeb, H.; Dharan, R.; Levi-Kalisman, Y.; Metanis, N.; Ringel, I.; Raviv, U., Effect of tubulin self-association on GTP hydrolysis and nucleotide exchange reactions. *Biochimica et Biophysica Acta (BBA)-Proteins and Proteomics* **2023**, *1871* (2), 140869.